Talanta 116 (2013) 330–334

Contents lists available at ScienceDirect

Talanta

journal homepage: www.elsevier.com/locate/talanta

# Long-tail probe-mediated cycled strand displacement amplification: Label-free, isothermal and sensitive detection of nucleic acids

Hongyan Su [a], Jiabao Long [a], Qiuping Guo [a], Xiaochun Meng [b], Yongjun Tan [a], Qingyun Cai [a], Zhuo Chen [a], Xiangxian Meng [a,*]

[a] College of Biology, State Key Laboratory of Chemo/Biosensing and Chemometrics, College of Chemistry and Chemical Engineering, Hunan University, Changsha 410082, China
[b] Department of Traditional Chinese Medicine, The Fourth Hospital of Changsha, Changsha 410006, China

ARTICLE INFO

*Article history:*
Received 7 February 2013
Received in revised form
6 May 2013
Accepted 11 May 2013
Available online 30 May 2013

*Keywords:*
Long-tail probe
Isothermal
Cycled strand displacement amplification
Label-free

ABSTRACT

We design a long-tail shaped DNA probe for the label-free, isothermal and sensitive detection of nucleic acids based on cycled strand displacement amplification (Ltail-CSDA). The long-tail probe, a stem-loop structure with a long poly(T) tail at 5′-termini, integrates target-binding and amplification and signaling within one multifunctional design. The specific binding between the long-tail probe and the target triggers a polymerization reaction, during which a long dsDNA product is synthesized and the hybridized target is displaced by the strand displacement activity of polymerase. The displaced target forms another specific probe-target binding and prompts cycled polymerization reactions. The proposed Ltail-CSDA has the distinct advantages of its isothermal nature, free-label, simplicity and attomolar sensitivity compared with other existing technologies. More significantly, the dynamic range of the method is extremely large, covering nine orders of magnitude. Using total RNA samples extracted from hepatitis C virus (HCV) as targets, we further demonstrate the detection capability of the method for complex nucleic acid samples, indicating its potential applicability for clinic molecular diagnostic assays.



## 1. Introduction

The invention of polymerase chain reaction (PCR) revolutionizes medical molecular diagnostics that rely on detecting and quantifying nucleic acid targets of interest [1]. Its applications to genetic analysis, DNA cloning, in vitro diagnosis, rapid screening of infectious diseases and others have been already well documented [2–4]. However, the requirement of precise control of temperature cycling and the resultant instrumental restraint has been hampering its wider and more versatile applications. There is a continuous demand in developing isothermal approaches for sensitive and convenient DNA detection.

Accordingly, various strategies for the nucleic acid detection were proposed, such as pyrene-excimer probes [5], enzyme conjugates [6,7], rolling circle amplification [8,9], locked nucleic acid (LNA)-based northern blot [10] and microarray-based flow cytometry [11]. These strategies involved methodological improvement in designing and labeling of primers or probes, chemical modification of nucleotides and incorporation of signal amplification. Notably, polymerase-based strand displacement amplification (SDA) has become increasingly popular in the detection of nucleic acids as a result of its robustness, specificity and isothermality [12–17]. Park et al. reported a SDA-based colorimetric method for DNA detection combined with RNase H [13,14]. However, rigorous optimizations are necessary for the activities of the polymerization of polymerase and the cleavage of RNase H in the same solution. Ward et al. developed a RNase H-free SDA-based method for detection of plant pathogens by introducing four to six primers' reactions [15]. Guo et al. proposed the cycled SDA method using molecular beacon, reaching a DNA target detection limit of 6.4 fM [16]. However, the multi-primers make their experimental design very sophisticated, and the double-labeled probes would make DNA detection quite expensive.

In this work, we designed a novel long-tail probe to perform label-free, simple, low-cost and isothermal detection of nucleic acids with high sensitivity and wide dynamic range based on target-triggered cycled SDA. We named the method as long-tail probe-mediated cycled SDA (Ltail-CSDA). The long-tail probe is a stem-loop structure DNA with a long poly(T) tail at 5′-termini and integrates target-binding, amplification and signaling within one multifunctional design. We reached the aims of the detection limit of 50 aM and the dynamic range of nine orders of magnitude relying on cycled SDA and the extensive polymerization products.

* Corresponding author. Tel./fax: +86 731 88887861.
*E-mail address:* xxmeng@hnu.edu.cn (X. Meng).

0039-9140/$ - see front matter © 2013 Elsevier B.V. All rights reserved.
http://dx.doi.org/10.1016/j.talanta.2013.05.021

## 2. Experimental section

### 2.1. Materials

Long-tail probes and other oligos were commercially synthesized by TaKaRa Bio Inc. (Dalian, China). Sequences of these oligos were listed in Tables S1 and S2 in the Supporting information. Polymerase klenow fragment exo$^-$ (KF$^-$) was purchased from New England Biolabs, Inc. The 10,000 × SYBR Green I (SG) was purchased from Invitrogen (CA, USA). The deoxynucleotide solution mixture (dNTPs) was purchased from TaKaRa Bio Inc. All other reagents were of analytical grade. Deionized water was obtained from the Nanopure Infinity™ ultrapure water system (Barnstead/Thermolyne Corp., Dubuque, IA, USA). 0.1% DEPC water was prepared for RNA experiments. The total RNA samples extracted from HCV were obtained from Ambion (Austin, USA).

### 2.2. Polymerization reaction catalyzed by polymerase KF$^-$

Unless specified, the experiments were performed in 100 μl solution consisting of $5 \times 10^{-10}$ M target, $5 \times 10^{-8}$ M long-tail probe2 and a basal solution, which contained 20 mM Tris–HCl (pH 7.9), 10 mM $MgCl_2$, 10 mM NaCl, 1 mM DTT, 5 U KF$^-$, 100 μM dNTPs and 50 nM primer. These samples were incubated at 37 °C for 2 h, and then heated at 85 °C for 5 min to inactivate KF$^-$. According to variant experiments, the concentration of the target and the type of the probe were adjusted. Additionally to investigate the influence on polymerization, we adjusted the concentrations of dNTPs, KF$^-$, $MgCl_2$, NaCl and DTT, and the polymerization time interval.

### 2.3. Fluorescence measurement

Polymerization product was mixed with 10 μl 10 × SG dye. The fluorescence intensities were recorded using F-2500 fluorescence spectrophotometer (Hitachi, Japan) with an aqueous thermostat (Amersham) accurate to 0.1 °C. The fluorescent spectra were measured using the spectrofluorophotometer. The excitation wavelength was 497 nm, and the spectra were recorded between 507 and 650 nm. The fluorescence emission intensity was measured at 530 nm.

### 2.4. Gel electrophoresis

Polymerization products were analyzed by a 20% non-denaturing PAGE, which was carried out in 1 × TBE (pH 8.3) at 80 V constant voltage for about 3 h. Bands were analyzed under the silver-straining method using an Image Master VDS-CL (Amersham Biosciences).

## 3. Results and discussion

### 3.1. Principle of Ltail-CSDA

The design of long-tail-mediated, label-free and isothermal detection for nucleic acids is illustrated (Fig. 1). The detection system consists of a long-tail probe, a short primer and polymerase. The long-tail probe contains three domains, a stem domain (SD), a long-tail domain (LTD) and a target-binding domain (TBD). The SD is 10-nt-long two complementary sequences, of which one strand at the 3′-end is matched to a 9-nt-long primer. The LTD, a long poly(T) sequence at the 5′-end, extends the length of dsDNA products when polymerization is triggered. The 4-nt poly(T) at the 3′-end prevents probe's own polymerization reaction. The TBD is where the specific binding occurs between the probe and the target. In the presence of the target Fig. 1b), the TBD-target binding undergoes a conformational change, leading to the stem separation of the SD (Step 1). Then, the primer anneals with the open stem and triggers a polymerization reaction in the presence of dNTP/polymerase (Step 2). Notably, during the primer extension, a long dsDNA product is synthesized and the hybridized target is displaced by the strand displacement activity of polymerase (Step 3). The displaced target hybridizes with another long-tail probe, triggering another polymerization reaction (Step 4) to generate a large number of long dsDNA polymerization products. Thus, fluorescent dye (SYBR green I, SG) preferably binds to the dsDNA products via intercalation [18], and leads to strong fluorescence signals, which is directly proportional to the concentrations of the target. In the absence of the target, there is no polymerization reaction and the long-tail probe keeps the hairpin structure and leads to weak fluorescence background (Fig. 1a).

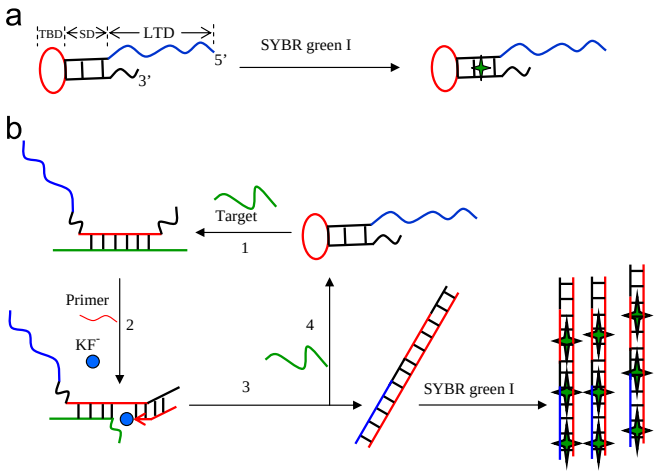


**Fig. 1.** Reaction mechanism of Ltail-CSDA. (a) In the absence of the target, the long-tail probe keeps hairpin structure and leads to weak fluorescence background. (b) In the presence of the target, the binding between the probe with the target undergoes a conformational change, leading to the stem separation of the probe (Step 1). A primer anneals with the open stem and triggers a polymerization reaction in the presence of dNTP/polymerase (Step 2). A long polymerization product is synthesized and the hybridized target is displaced by polymerase in the process of primer extension (Step 3). The displaced target hybridizes with another long-tail probe, and triggers another polymerization reaction (Step 4). Cycled polymerization amplification produces a large number of long dsDNA products, leading to strong fluorescence along with the intercalation of SG molecules.

The dsDNA polymerization products were quantified via the fluorescence intensity of SG. We reason that the long-tail probe could improve both the sensitivity and the specificity of nucleic acid detection. The fact that long polymerization products resulting from the long-tail probe can bind more molecules of SG and offer additional signal amplification for nucleic acid detection. Moreover, the presence of the hairpin structures in the long-tail probe brings about high conformational constraint, and the competition between the stem region and the loop/target binding could significantly improve the specificity [8,19–23].

### 3.2. Design of the long-tail probe

To achieve the desired degree of amplification, our design relies upon both the annealing of the primer with the long-tail probe and the length of dsDNA polymerization products. From the principle of Ltail-CSDA (Fig. 1), the long-tail probe in the study must have a stem long enough to ensure that stem hybridization affinity will be stronger than hybridization affinity with the primer, in order to prevent polymerization reaction in the absence of the target. On the other hand, the stem cannot be too long as it may restrain the conformational change of the probe when

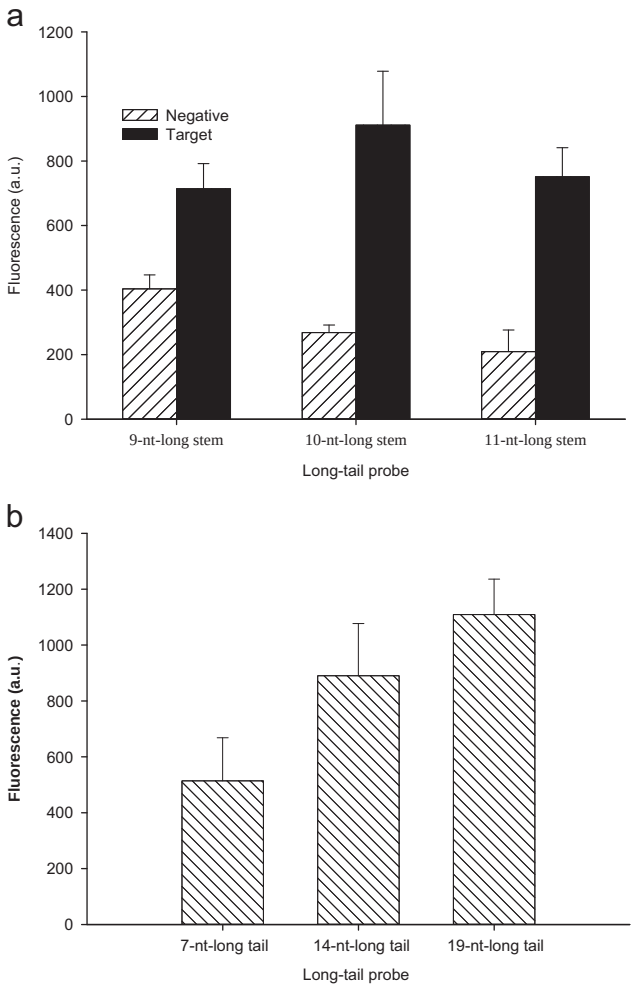


**Fig. 2.** The design of long-tail probes. (a) Three long-tail probes with 9, 10 or 11-nt-long stem were performed in the absence of target (negative samples) or in the presence of $5 \times 10^{-12}$ M target (target samples). (b) Three long-tail probes with 7, 14 or 19-nt-long tail were performed in the presence of $5 \times 10^{-12}$ M target. Data were collected from at least three independent sets of experiments. Error bars (SD) were estimated from at least three independent measurements.

hybridizing with its targets. Hence, in this work, three long-tail probes (long-tail probe1, 2 and 3, Table S1) with 9, 10 or 11-nt-long stem respectively, were firstly investigated in the absence or the presence of the target. These probes with different length of stems have the same 14-nt-long poly(T) tails. In the absence of the target, it was found that 10 and 11-nt-long stem probes had obvious lower fluorescence signals compared with 9-nt-long stem probe did. While in the presence of the target, 10-nt-long stem probes had significantly stronger fluorescence signals compared with 9 or 11-nt-long stem probes did (Fig. 2a). This indicated that the 10-nt-long stem probe probably formed a structure stable enough to effectively prevent the primer from annealing with duplex stem in the absence of the target; at the same time, the probe was convenient to conformational change in the presence of the target. Then, three long-tail probes (long-tail probe 2, 4, and 5, Table S1) with 7, 14 or 19-nt-long tail respectively, were investigated in the presence of the target. These probes with different lengths of tails have the same 10-nt-long stems. It was found that fluorescence intensity obviously enhanced as the length of tails increased (Fig. 2b). The reason probably was that long dsDNA polymerization products resulting from probes with a long poly(T) tail inserted more SG dye than short polymerization products from probes with a short poly(T) tail did. The polymerization products were further confirmed by electrophoresis (Fig. S1 in the Supporting information).

### 3.3. Factors affecting polymerization process

The polymerization process can be affected by many molecular species including biomolecules and metal ions [9,24]. The effects of polymerization time, dNTP, $KF^-$ and magnesium metal ion have been studied (Fig. 3). The fluorescence signal was calculated as $[(F-F_{buffer})-(F_0-F_{buffer})]/(F_0-F_{buffer})$, in which $F_{buffer}$ was the fluorescence intensity of the solution without both SG and the target, $F_0$ was the fluorescence intensity of the solution with SG and without the target, and $F$ was the fluorescence intensity of the solution with both SG and the target. It was found that the fluorescence signal enhanced with the increase of the polymerization time (Fig. 3a), indicating that the continuous formation of products was the result of cycled polymerization reaction. Electrophoresis results (Fig. S1) also perfectly demonstrated the formation of polymerization products in different polymerization time intervals. It was also found that the polymerization did not take place unless dNTP, $KF^-$ or magnesium ion was added to the polymerization mixture (Fig. 3b–d). The signal reached its maximum rate at 200 μM dNTP, 5 U $KF^-$ and 20 mM magnesium ion. Too low concentration of dNTP (20 μM) and $KF^-$ (0.5 U) obviously hindered the polymerization reaction, probably due to the decrease of the polymerization efficiency [9]. Magnesium ion, as an activator of many enzymes [25–27], is essential for polymerization reaction. However, too high concentration of magnesium ion would significantly decrease the signal as demonstrated in Fig. 3d, indicating an obvious inhibition on polymerization reaction. The effects of DTT and sodium ion were also studied, suggesting a similar inhibition at their high concentrations similar to magnesium ion (data not shown).

### 3.4. Detection of target with high sensitivity

In a set of further experiments, we investigated the sensitivity of Ltail-CSDA in optimized conditions. Various concentrations of targets were detected using Ltail-CSDA (Fig. 4, Fig. S2 in the Supporting information). The fluorescence intensity increased upon addition of the target to the mixture containing dNTPs and polymerase, indicating that the polymerization reaction was triggered by the target. Furthermore, the fluorescence intensity gradually increased along with the target concentration, leading to an impressive large dynamic range that spanned nine orders of magnitude (50 aM to 50 nM). The fluorescence signal was significantly larger than the background ($P < 0.05$), even when the concentration of the target was as low as 50 aM ( $> 3$ SD; the inset of Fig. 4), which indicated that the detection limit of Ltail-CSDA was at least 50 aM. The method remarkably improved the sensitivity by two orders of magnitude compared with previously proposed molecular beacon-mediated cycled SDA [16]. Further, we compared the Ltail-CSDA with traditional probe-mediated CSDA to reveal the advantages of our proposed method. Without poly(T) tail, the traditional probe here designed (Table S1) has the similar sequences as long-tail probe2. As observed for traditional probe, the signal was very low until the target concentration reached 500 fM (Fig. S3 in the Supporting information), indicating the detection limit was 500 fM. In this regard, the novel Ltail-CSDA has remarkable sensitivity improvement by four orders of magnitude compared with traditional probe-mediated CSDA. Notably, it was also found in the same concentrations of the target that fluorescence intensity of Ltail-CSDA was significant stronger than that of traditional probe-mediated CSDA. The high sensitivity and strong fluorescence intensity of Ltail-CSDA probably should be due to the formation of 53-nt-long dsDNA polymerization products in Ltail-CSDA, while only 39-nt-long dsDNA polymerization products in traditional probe-mediated CSDA. Furthermore, the sensitivity

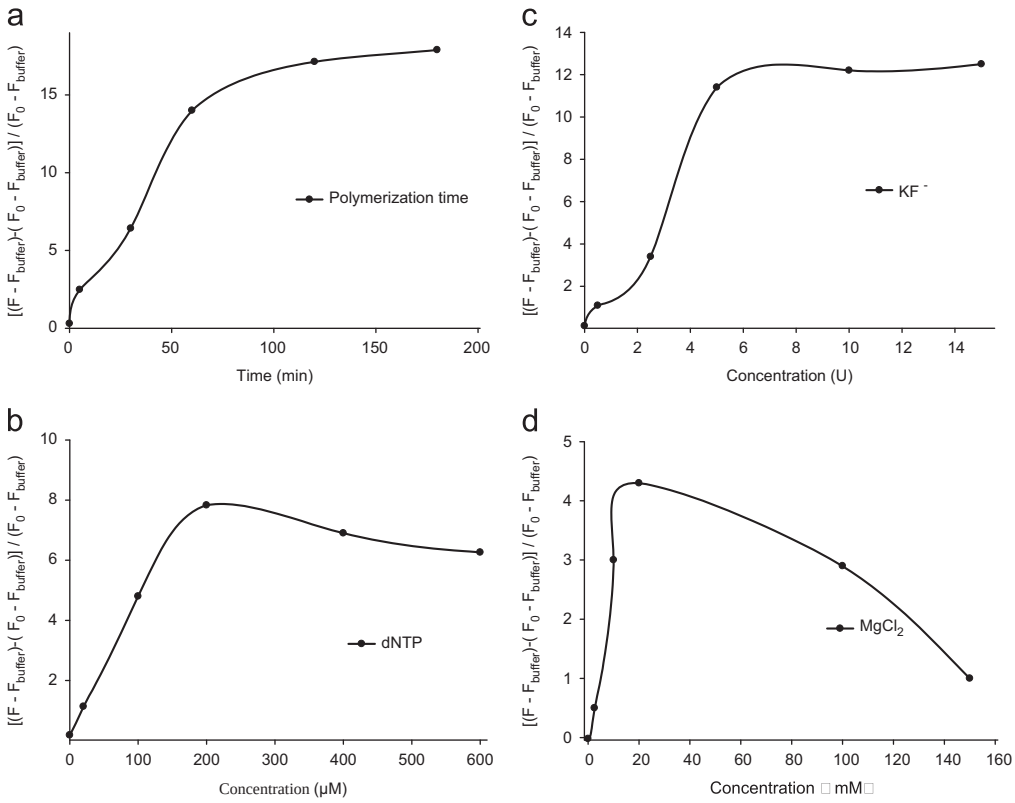


**Fig. 3.** Effects of molecular species on polymerization process in the presence of $5 \times 10^{-12}$ M target. (a) Effects of reaction time on polymerization reaction. (b) Effects of dNTP on polymerization. (C) Effects of $KF^-$ on polymerization. (d) Effects of magnesium ion on polymerization. The fluorescence signal is calculated as $[(F–F_{buffer})–(F_0–F_{buffer})]/(F_0–F_{buffer})$, in which $F_{buffer}$ is the fluorescence intensity of buffer solution without both SG and the target, $F_0$ is the fluorescence intensity of the solution with SG and without the target, and $F$ is the fluorescence intensity of the solution with both SG and the target.

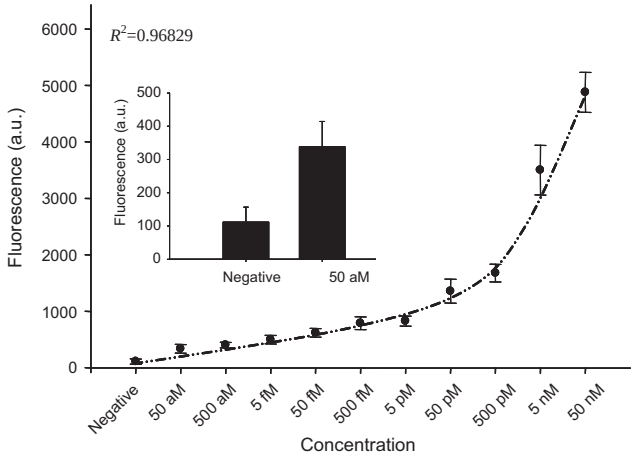


**Fig. 4.** The detection performance by Ltail-CSDA. The concentration profile for the detection of target was in the range from 50 aM to 50 nM. Data were collected from at least three independent sets of experiments. Error bars (SD) were estimated from at least three independent measurements. The squared correlation coefficient ($R^2$) was analyzed by sigmoidal fit.

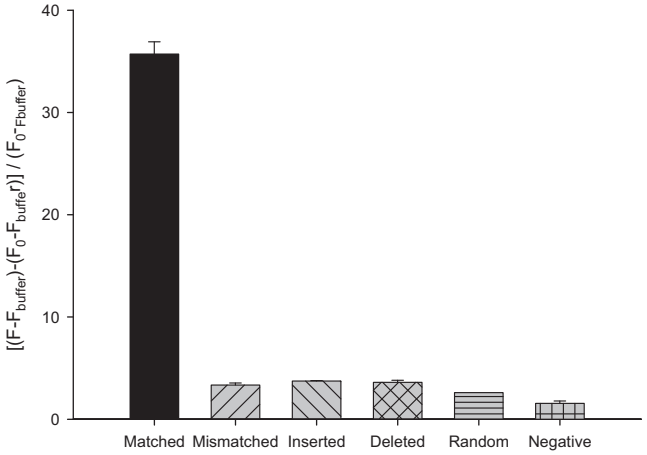


**Fig. 5.** Response of long-tail probe to a matched target, mismatched, deleted, inserted and random DNAs. The fluorescence signal is calculated as $[(F–F_{buffer})–(F_0–F_{buffer})]/(F_0–F_{buffer})$, in which $F_{buffer}$ is the fluorescence intensity of buffer solution without both SG and the target, $F_0$ is the fluorescence intensity of the solution with SG and without the target, and F is the fluorescence intensity of the solution with both SG and the target. Data were collected from at least three independent sets of experiments. Error bars (SD) were estimated from at least three independent measurements.

of the proposed method would be further improved by using longer poly(T) tail probes.

### 3.5. *Selectivity of Ltail-CSDA*

Then, we used various oligos as matched, mismatched, deleted, inserted and random DNAs to investigate the specificity of Ltail-CSDA. The matched was the target, complementary to the long-tail probe. The mismatched was a single base different from the matched target. The deleted and inserted DNAs were a deleted nucleotide or an inserted nucleotide compared with the matched target (Table S2). The fluorescence signal was significantly larger in the solution containing matched target than that of in the negative samples with mismatched, deleted, inserted and random DNAs (Fig. 5). This probably indicated a high specificity of Ltail-CSDA, which the matched target prompted effectively the cycled polymerization reaction, while negative samples did not.

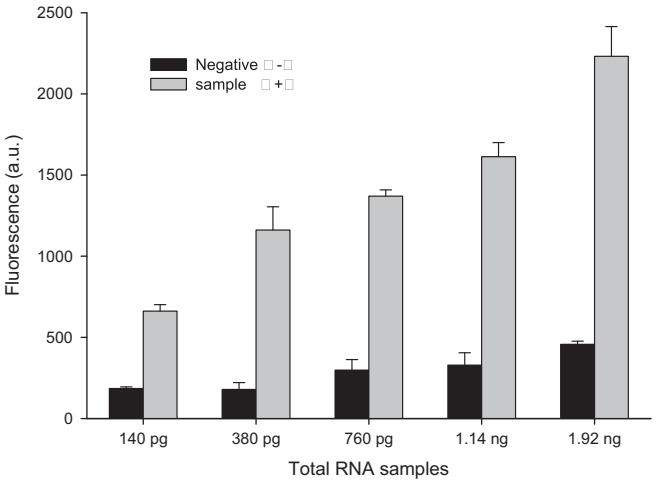


**Fig. 6.** The detection of total RNA samples extracted from hepatitis C virus (HCV-RNA) using Ltail-CSDA. Negative control (−) was performed with identical conditions in total RNA samples (+) without adding polymerase $KF^-$. Data were collected from at least three independent sets of experiments. Error bars (SD) were estimated from at least three independent measurements.

### 3.6. Detection of the total RNA sample of HCV

Given the high sensitivity, sequence specificity and large dynamic range of Ltail-CSDA, we attempted to employ this novel strategy to perform not only DNA detection, but also RNA analysis, even complex virus RNA analysis. Using total RNA samples extracted from hepatitis C virus (HCV-RNA) as targets, we demonstrated the detection capability of Ltail-CSDA for complex nucleic acid samples. HCV-RNA is a 9600-nt positive sense single-stranded RNA genome [28]. We employed Ltail-CSDA to detect total RNA samples extracted from HCV. The samples and negative controls were performed either in the presence or the absence of $KF^-$. We found that the fluorescence intensity enhanced along with the increase of the concentration of HCV-RNA (Fig. 6). It is important to note that our Ltail-CSDA method can reliably detect directly in total RNA samples as few as 140 pg, which would probably provide a feasible approach for clinical diagnostics. However, the detection sensitivity of Ltail-CSDA for the total RNA samples is not sufficient for direct detection of clinic samples, and, as a result, a pretreatment, such as enrichment, may be necessary for direct detection of clinic biological samples.

## 4. Conclusions

In summary, the Ltail-CSDA strategy was presented for the label-free, simple-operated, isothermal and low-cost detection of nucleic acids with a target detection limit to 50 aM. The advantages of the Ltail-CSDA include: (i) Design is facile. The long-tail probe integrates target-binding, amplification and signaling within one multifunctional design; (ii) the sensitive detection of Ltail-CSDA results from amplification of cycled polymerization reaction and extension of polymerization products. More significantly, the dynamic range of Ltail-CSDA is extremely large, covering nine orders of magnitude; (iii) Ltail-CSDA is an isothermal amplification protocol that does not rely on expensive devices, which significantly reduces the cost of Ltail-CSDA assays. We expect that this highly sensitive and inexpensive Ltail-CSDA will have high applicability in the nucleic acid detection method in clinical diagnostics.

## Acknowledgment

This work was supported by the National Natural Science Foundation of China (21275043) and National Basic Research Program of China under Grant 2009CB421601.

## Appendix A. Supporting information

Supplementary data associated with this article can be found in the online version at http://dx.doi.org/10.1016/j.talanta.2013.05.021.

## References

[1] R.K. Saiki, S. Scharf, F. Faloona, K.B. Mullis, G.T. Horn, H.A. Erlich, N. Arnheim, Science 230 (1985) 1350–1354.
[2] C. Chen, D.A. Ridzon, A.J. Broomer, Z. Zhou, D.H. Lee, J.T. Nguyen, M. Barbisin, N.L. Xu, V.R. Mahuvakar, M.R. Andersen, Nucleic Acids Res. 33 (2005) e179.
[3] P.P. Banada, S. Chakravorty, D. Shah, M. Burday, F.M. Mazzella, D. Alland, PLOS One 7 (2012) e31126.
[4] C.K. Raymond, B.S. Roberts, E.P. Garrett, L.P. Lim, J.M. Johnson, RNA 11 (2005) 1737–1744.
[5] J. Huang, Y.R. Wu, Y. Chen, Z. Zhu, X.H. Yang, C.Y. Yang, K.M. Wang, W.H. Tan, Angew. Chem. Int. Ed. 50 (2011) 401–404.
[6] F. Patolsky, A. Lichtenstein, I. Willner, Nat. Biotechnol. 19 (2001) 253–257.
[7] D.J. Caruana, A.J. Heller, Am. Chem. Soc. 121 (1999) 769–774.
[8] Y.T. Zhou, Q. Huang, J.M. Gao, J.X. Lu, X.Z. Shen, C.H. Fan, Nucleic Acids Res. 38 (2010) e156.
[9] T. Murakami, J. Sumaoka, M. Komiyama, Nucleic Acids Res. 37 (2009) e19.
[10] A. Valoczi, C. Hornyik, N. Varga, J. Burgyan, S. Kauppinen, Z. Havelda, Nucleic Acids Res. 32 (2004) e175.
[11] J.M. Thomson, J. Parker, C.M. Perou, S.M. Hammond, Nat. Methods 1 (2004) 47–53.
[12] F. Xuan, X. Luo, I.M. Hsing, Biosens. Bioelectron. 35 (2012) 230–234.
[13] H.G. Park, C. Jung, J.W. Chung, U.O. Kim, M.H. Kim, Biosens. Bioelectron. 26 (2011) 1953–1958.
[14] H.G. Park, C. Jung, J.W. Chung, U.O. Kim, M.H. Kim, Anal. Chem. 82 (2010) 5937–5943.
[15] L.I. Ward, S.J. Harper, Methods Mol. Biol. 862 (2012) 161–170.
[16] Q.P. Guo, X.H. Yang, K.H. Wang, W.H. Tan, W. Li, H.X. Tang, H.M. Li, Nucleic Acids Res. 37 (2009) e20.
[17] H. Dong, J. Zhang, H. Ju, H. Lu, S. Wang, S. Jin, K. Hao, H. Du, X. Zhang, Anal. Chem. 84 (2012) 4587–4593.
[18] H. Zipper, H. Brunner, J. Bernhagen, F. Vitzthum, Nucleic Acids Res. 32 (2004) e103.
[19] S. Tyagi, F.R. Kramer, Nat. Biotechnol. 14 (1996) 303–308.
[20] H.H. El, S.A. Marras, S. Tyagi, E. Shashkina, M. Kamboj, T.E. Kiehn, M.S. Glickman, F.R. Kramer, D. Alland, J. Clin. Microbiol. 47 (2009) 1190–1198.
[21] S. Tyagi, D.P. Bratu, F.R. Kramer, Nat. Biotechnol. 16 (1998) 49–53.
[22] W.J. Kang, Y.L. Cho, J.R. Chae, J.D. Lee, K.J. Choi, S. Kim, Biomaterials 32 (2011) 1915–1922.
[23] A. Dai, W. Yang, E. Firlar, S.A. Marras, M. Libera, Soft Matter 8 (2012) 3067–3076.
[24] X.X. Meng, R.B. Luan, K.M. Wang, X.H. Yang, Q.P. Guo, Life Sci. Res. 11 (2007) 230–295.
[25] N.E. Grochowska, B. Calyniuk, W.M. Muc, Z.E. Nowakowska, J. Biol. Regul. Homeost. Agents 26 (2012) 763–767.
[26] Y. Sun, S. Selvaraj, A. Varma, S. Derry, A.E. Sahmoun, B.B. Singh, J. Biol. Chem. 288 (2013) 255–263.
[27] Z.W. Tang, K.M. Wang, W.H. Tan, C.B. Ma, J. Li, L.F. Liu, Q.P. Guo, X.X. Meng, Nucleic Acids Res. 33 (2005) e97.
[28] J. Cohen, Science 285 (1999) 26–30.